1 The response of linear reservoirs to periodic forcing

The derivations in 1.1-1.3 and the resulting equations are not novel. We think, however, that presenting them altogether might be a useful overview for the interested reader. General overviews on linear systems theory are given for example by Dooge (1973) for hydrology or by Smith (2007) for signal processing. The response of linear reservoirs to periodic forcing was for example described by Eriksson (1971) or Peters et al. (2003).

1.1 Single linear reservoir

The outflow Q from a linear reservoir is described by Equation (S.1):

$$Q = \frac{S}{\tau} \tag{S.1}$$

Conservation of mass requires that the rate of change of storage S equals the inflow Q_{in} minus the outflow Q from the reservoir:

$$\frac{dS}{dt} = Q_{\text{in}} - Q \tag{S.2}$$

For simplicity, we consider a simple sinusoidal input signal with unit amplitude, with a phase of zero (i.e. aligned with the cycle of interest) and with zero mean. We also replace the period T by the angular frequency $\omega = \frac{2\pi}{T}$.

$$Q_{\text{in}}(t) = \sin(\omega t) \tag{S.3}$$

Combining Equations (S.1), (S.2), and (S.3) yields:

$$\frac{dQ}{dt} + \frac{Q}{\tau} = \frac{\sin(\omega t)}{\tau} \tag{S.4}$$

which is a first-order ordinary differential equation (ODE) that can be solved with the help of an integrating factor $\exp(t/\tau)$ and by using the product rule:

$$\exp\left(\frac{t}{\tau}\right)\left(\frac{dQ}{dt} + \frac{Q}{\tau}\right) = \exp\left(\frac{t}{\tau}\right)\frac{\sin(\omega t)}{\tau} \tag{S.5}$$

$$\frac{d}{dt}\left(\exp\left(\frac{t}{\tau}\right)Q\right) = \exp\left(\frac{t}{\tau}\right)\frac{\sin(\omega t)}{\tau} \tag{S.6}$$

$$\left[\exp\left(\frac{t}{\tau}\right)Q\right]_0^t = \frac{1}{\tau}\int_0^t \exp\left(\frac{t}{\tau}\right)\sin(\omega t)dt \tag{S.7}$$

$$\exp\left(\frac{t}{\tau}\right)Q(t) - Q(0) = \frac{1}{\tau}\int_0^t \exp\left(\frac{t}{\tau}\right)\sin(\omega t)dt \tag{S.8}$$

Since we are interested in the steady-state periodic response of our system, we set $Q(0) = 0$. We can solve the integral on the right hand side using an integration rule (see e.g. Spiegel, 1968):

$$\exp\left(\frac{t}{\tau}\right)Q(t) = \frac{1}{\tau}\frac{\exp\left(\frac{t}{\tau}\right)}{\sqrt{(\frac{1}{\tau})^2 + \omega^2}}\sin\left(\omega t + \arccos\left(\frac{1}{\tau}\frac{1}{\sqrt{(\frac{1}{\tau})^2 + \omega^2}}\right)\right) \tag{S.9}$$

$$Q(t) = \frac{1}{\sqrt{1 + (\omega\tau)^2}} \sin\left(\omega t + \arccos\left(\frac{1}{\sqrt{1 + (\omega\tau)^2}}\right)\right) \qquad \text{(S.10)}$$

If we rewrite $A = \frac{1}{\sqrt{1+(\omega\tau)^2}}$ (Equation (9) in the corresponding manuscript) and $\phi = \arccos(A)$ (Equation (10) in the corresponding manuscript), we obtain:

$$Q(t) = A\sin(\omega t + \phi) \qquad \text{(S.11)}$$

Since the system is linear, other inflow amplitudes can be accounted for by scaling (multiplication) and non-zero offsets by addition. We could also superimpose other inputs of different periods. Note that we can obtain the same result using the transfer function approach in linear systems theory, as for example described in Dooge (1973) or Smith (2007).

1.2 Linear reservoirs in series

Linear reservoirs in series can be conceptualised as follows. The outflow from the first reservoir is the inflow to the second reservoir, the outflow from the second reservoir is the inflow to the third reservoir, and so forth. Let's denote the outflow from the first reservoir by Q_1:

$$Q_1(t) = A_1 \sin(\omega t + \phi_1) \qquad \text{(S.12)}$$

If we use Equation (S.12) as inflow to the second reservoir (which is also the total outflow), we obtain:

$$\frac{dQ_2}{dt} + \frac{Q_2}{\tau_2} = \frac{A_1 \sin(\omega t + \phi_1)}{\tau_2} \qquad \text{(S.13)}$$

This can be solved in a similar fashion as before (Equation (S.4)) and we get:

$$Q_2(t) = A_1 A_2 \sin(\omega t + \phi_1 + \phi_2) \qquad \text{(S.14)}$$

If we continue to do this for n reservoirs, we get:

$$Q_n(t) = A_1 A_2 \ldots A_n \sin(\omega t + \phi_1 + \phi_2 + \ldots + \phi_n) \qquad \text{(S.15)}$$

$$Q_n(t) = \prod_{i=1}^{n} A_i \sin\left(\omega t + \sum_{i=1}^{n} \phi_i\right) \qquad \text{(S.16)}$$

The total amplitude ratio is thus obtained by multiplication of all individual amplitude ratios and the total phase shift by addition of all individual phase shifts. If all the reservoirs have the same time constant ($\tau_1 = \tau_2 = \cdots = \tau_n$), we obtain the so called Nash cascade (Nash, 1957).

1.3 Linear reservoirs in parallel

Linear reservoirs in parallel are the weighted sum of the outflow from each reservoir. The resulting flow is hence a sum of sine waves of the same angular frequency, weighted by the fraction p_i going into each reservoir. For two reservoirs we can write:

$$Q_{12}(t) = Q_1(t) + Q_2(t) \qquad \text{(S.17)}$$

where Q_{12} is the combined outflow from the two reservoirs Q_1 and Q_2. We can use Equation (S.11) to get the outflow from each of the two reservoirs:

$$Q_{12}(t) = p_1 A_1 \sin(\omega t + \phi_1) + p_2 A_2 \sin(\omega t + \phi_2) \tag{S.18}$$

The sum of two sine waves (Equation (S.18)) can be rewritten to obtain only one sine wave:

$$Q_{12}(t) = p_1 A_1 \sin(\omega t + \phi_1) + p_2 A_2 \sin(\omega t + \phi_2) \tag{S.19}$$
$$Q_{12}(t) = A_{12} \sin(\omega t + \phi_{12}) \tag{S.20}$$

where the total amplitude ratio A_{12} (Equation (14) in the corresponding manuscript) and the total phase shift ϕ_{12} (Equation (15) in the corresponding manuscript) are given by (see e.g. Smith, 2007):

$$A_{12} = \sqrt{[p_1 A_1 \cos \phi_1 + p_2 A_2 \cos \phi_2]^2 + [p_1 A_1 \sin \phi_1 + p_2 A_2 \sin \phi_2]^2} \tag{S.21}$$

$$\phi_{12} = \arctan\left(\frac{p_1 A_1 \sin \phi_1 + p_2 A_2 \sin \phi_2}{p_1 A_1 \cos \phi_1 + p_2 A_2 \cos \phi_2}\right) \tag{S.22}$$

We could do the same for more (n) reservoirs by stepwise adding the resulting sine wave to the next sine wave (e.g. $Q_{12} + Q_3$).

1.4   Non-linear reservoirs

Non-linear behaviour is frequently observed why many authors used non-linear reservoirs instead (e.g. Wittenberg, 1999). We therefore investigate how non-linear reservoirs respond to periodic inputs to see whether non-linear behaviour is invalidating our approach. A non-linear reservoir can be described by (Kirchner, 2009):

$$Q = Q_{\text{ref}} \left(\frac{S - S_0}{m}\right)^n \tag{S.23}$$

where Q_{ref} is an arbitrary reference discharge, S_0 is a reference storage, m is a scaling coefficient (it has the units of storage), and n is a non-linearity parameter ($n = 1$ results in the linear reservoir). For non-linear reservoirs, there are no general analytical solutions available. Non-linear reservoirs cannot be characterised by an invariant time constant, as their outflow rate depends on the storage, as it can be seen from Equation (S.23). Hence, we model the response of a single non-linear reservoir numerically.

The outflow from a non-linear reservoir forced by a sinusoidal input is shown in Figure S.1. The outflow is still periodic, but the "sine curve" is somewhat squeezed. This results in the maxima and minima not having the same distance and hence there is no unique phase shift. For the example shown in Figure S.1, the phase shift between the maxima of Q_{in} and Q_{out} is 68 days, and the phase shift between the minima is 70 days. The difference between the maximum amplitude and the mean amplitude (0.49 mm) is 0.20 mm, and the difference between the minimum amplitude and the mean amplitude is 0.18 mm. This asymmetry is partly due to numerical inaccuracies, however, probably mostly due to the non-linearity of the reservoir. Because non-linear reservoirs with $n > 1$ drain more slowly as they empty, their minima are closer to the mean and the minima have a larger phase shift (and vice versa for $n < 1$).
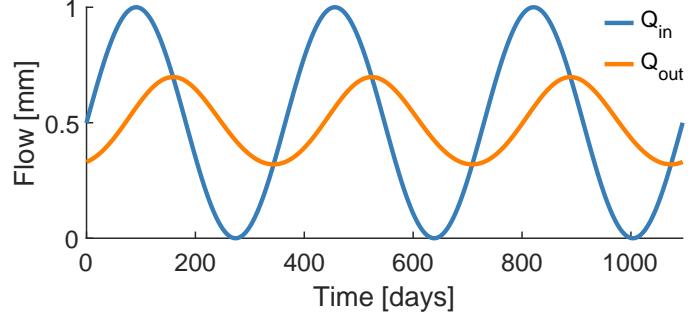
Figure S.1: Numerical approximation of steady-state (sinusoidal) inflow to and outflow from a non-linear reservoir ($Q_{\text{ref}} = 1$ mm, $S_0 = 0$ mm, $m = 200$ mm, $n = 2$). The starting time is chosen arbitrarily.

We can plot amplitude ratios and phase shifts for non-linear reservoirs with different parameter sets. We therefore do not need to specify a characteristic time constant. This is shown in Figure S.2. Even though the outflow is not exactly a sine wave, it is possible to define a mean phase shift and amplitude ratio, and in practice this might be a reasonably good approximation and hardly distinguishable from an actual sine wave. So, even if the reservoir is non-linear, its steady state behaviour (or the response to seasonal inputs) might be reasonably well approximated by a linear reservoir with a time constant that reflects the outflow characteristics at a characteristic storage level (e.g. mean storage).
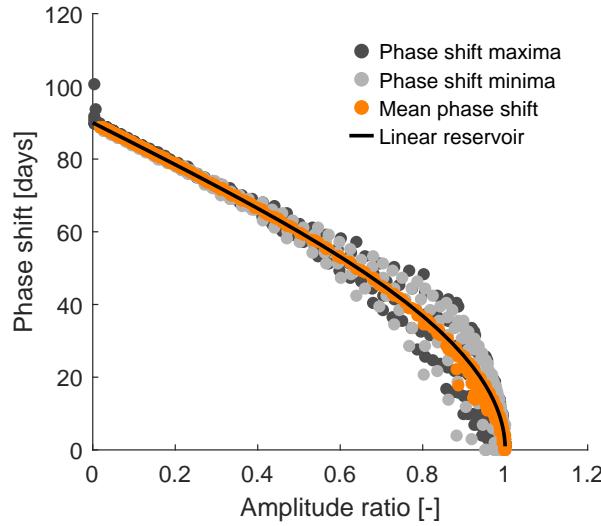
Figure S.2: Amplitude ratio and phase shift for a single non-linear reservoir for varying parameters sets. The phase shifts of the maxima, the minima, and the mean phase shifts are indicated by coloured dots. The non-linearity parameter n ranges from 0.5 to 10.

2 Additional analyses

2.1 Extracting seasonal components from time series

2.1.1 Comparison of fitting methods

We tested two methods to extract seasonal components from time series. The first method is a multiple linear regression. The second method makes use of the cross-covariance of two time series, which is described below.

2.1.2 Linear regression

A basic sine wave is given by:

$$x(t) = \delta_x \bar{x} \sin(2\pi \frac{t}{T} - \phi_x) + \bar{x} \tag{B.24}$$

We can rewrite Equation (B.24) as follows:

$$x(t) = \alpha \cos(2\pi \frac{t}{T}) + \beta \sin(2\pi \frac{t}{T}) + \bar{x} \tag{B.25}$$

We can solve for α, β and $\bar{x}$ in Equation (B.25) by means of multiple linear regression and then solve for δ_x and ϕ_x via the identities:

$$\delta_x \bar{x} = \sqrt{\alpha^2 + \beta^2} \tag{B.26}$$

$$\phi_x = \arctan\left(\frac{\beta}{\alpha}\right) \tag{B.27}$$

Note that the atan2(b, a) function is required to obtain an unambiguous phase shift.

2.1.3 Cross-covariance method

The unbiased estimate of the cross-covariance of two sine waves x and y is given by:

$$\gamma_{xy}(k) = \frac{1}{2}\delta_x \bar{x}\delta_y \bar{y} \cos\left((\phi_x - \phi_y) - 2\pi\frac{t}{T}k\right) \tag{B.28}$$

where k is the lag between the sine waves, $\delta_x \bar{x}$ and $\delta_y \bar{y}$ are their amplitudes, and ϕ_x and ϕ_y are their phase shifts. If we define x to be the signal of interest (e.g. streamflow) and y to be a dummy cycle of unit amplitude and zero initial phase shift ($\delta_y \bar{y} = 1$ and $\phi_y = 0$), Equation (B.28) simplifies to:

$$\gamma_{xy}(k) = \frac{1}{2}\delta_x \bar{x} \cos\left(\phi_x - 2\pi\frac{t}{T}k\right) \tag{B.29}$$

We can calculate the empirical cross-correlation between the two cycles and fit a sine curve to it (via nonlinear least squares). The parameters of that sine curve can then be used to find the parameters of our cycle of interest ($\delta_x \bar{x}$ and ϕ_x) via Equation (B.29).

The fitting methods (linear regression and cross-covariance method) show an almost perfect match (Figure S.3), which indicates that the extraction of the seasonal component is not sensitive to the method. While this means that we can reliably extract the sinusoidal component of the period of interest (1 year), it does not mean that we perfectly extracted the "(annual) seasonal component" of the variable of interest. A sine wave is just a parsimonious approximation of the seasonal behaviour and the choice of a sine wave to model seasonality is also associated with uncertainty.
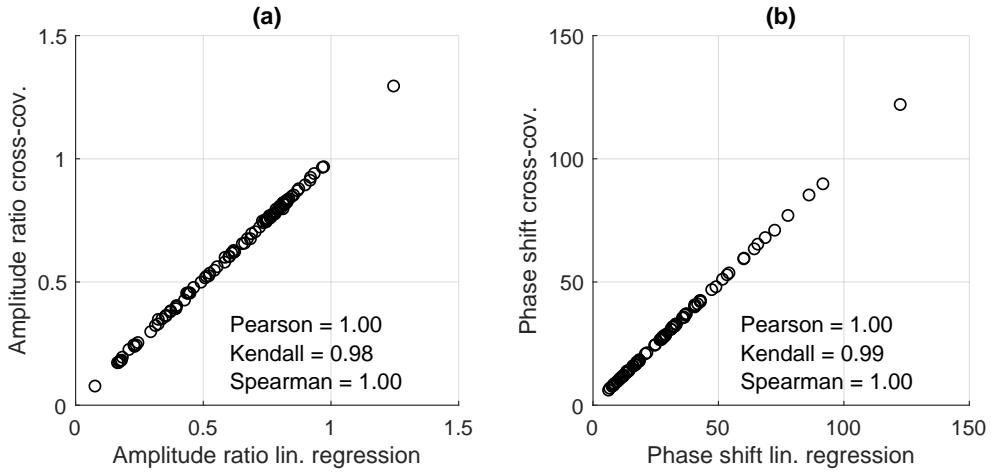
Figure S.3: Comparison of amplitude ratio **(a)** and phase shift **(b)** using the different sine fitting methods for UK catchments from 1989 to 2009. Note that both axes are limited.

2.1.4 Robustness of seasonal signatures

To check whether the seasonal signatures are robust, we calculate the signatures for two different time periods: from 1989 to 1999, and from 1999 to 2009.
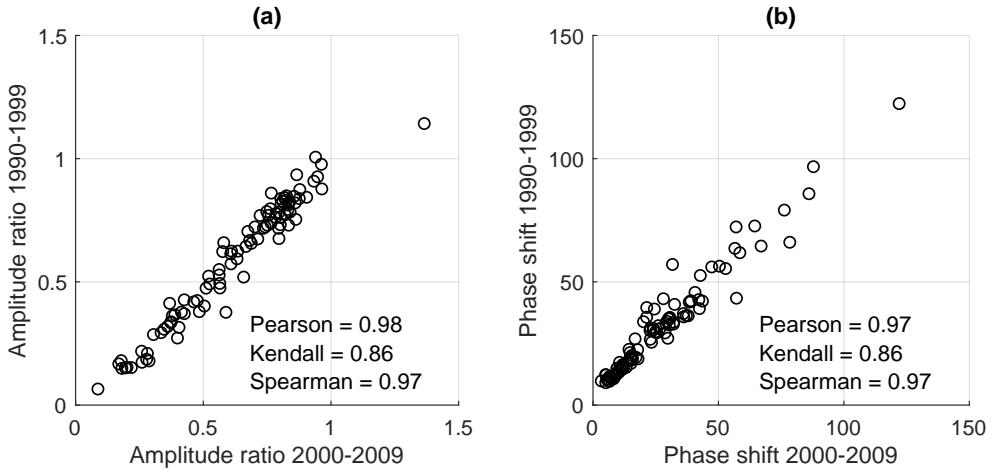
Figure S.4: Comparison of amplitude ratio **(a)** and phase shift **(b)** using different time periods for UK catchments. Note that both axes are limited.

Figure S.4 shows that the amplitude ratio and the phase shift show good agreement for the different time periods analysed. This means that the period from 1989 to 1999 does not exhibit a fundamentally different behaviour than the period from 1999 to 2009, i.e. the signatures are robust. A slight deviation can be expected as the forcing varies from year to year.

2.2 Catchments with precipitation falling as snow

Snow presents a different storage process that is not considered in the current approach. We therefore remove snowy catchments, defined as catchments with a snow fraction larger than 0.001, from the analysis. Figure S.5 shows the snowy catchments and the corresponding snow fraction.
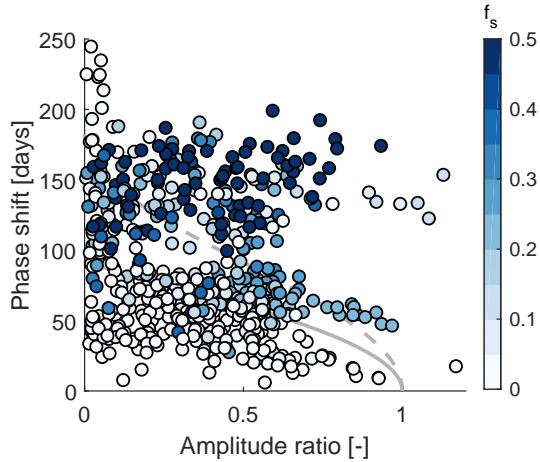
Figure S.5: Amplitude ratio against phase shift for CAMELS catchments. Colour indicates the fraction of precipitation falling as snow. Note that both axes are limited.

2.3 On the use of potential evapotranspiration as input signal

As mentioned in the corresponding manuscript, we use precipitation P minus potential evapotranspiration E_p as a proxy for the input signal to a catchment (the forcing F). This is motivated by its simplicity and the assumption that in energy-limited ($\bar{E}_p/\bar{P} < 1$) catchments actual evapotranspiration E_a is closely resembling potential evapotranspiration. Considering the annual water balance, all the catchments in the UK are energy-limited and a large fraction of catchments in the US are energy-limited. To test the validity of the assumption that $E_a = E_p$ in a rather straightforward manner, we adjust the seasonal component of E_p to obtain E_a by means of the Budyko framework (Budyko, 1974). We reduce the peak of the seasonal component of E_p so that it equals the mean of E_a, which we estimate using the following equation (Budyko, 1974):

$$\frac{\bar{E}_a}{\bar{P}} = \sqrt{\frac{\bar{E}_p}{\bar{P}} \tanh\left(\frac{\bar{P}}{\bar{E}_p}\right)\left(1 - \exp\left(-\frac{\bar{E}_p}{\bar{P}}\right)\right)} \tag{B.30}$$

We therefore obtain a new sine curve for the seasonal component of E_a, which has a reduced amplitude ($\delta_{E_a}\bar{E}_a$) and a reduced mean ($\bar{E}_a$), but the same phase as the sine curve for the seasonal component of E_p. This will increase the amplitude ratio and might change the phase shift whenever $\bar{E}_a < \bar{E}_p$.
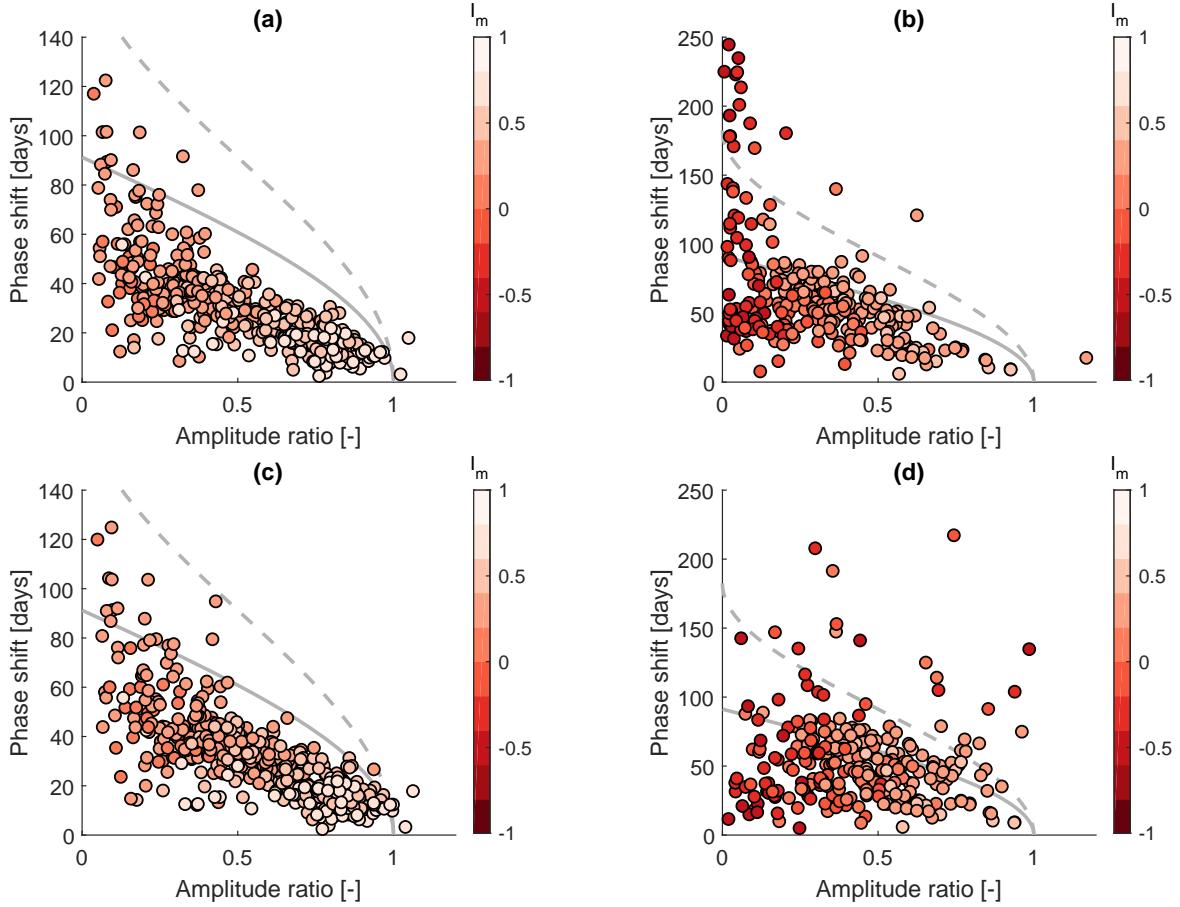
Figure S.6: Amplitude ratio against phase shift for **(a)** UK catchments and **(b)** CAMELS catchments using estimated actual evapotranspiration in the forcing ($F = P - E_a$) and for **(c)** UK catchments and **(d)** CAMELS catchments using potential evapotranspiration in the forcing ($F = P - E_p$). Grey solid line indicates a single linear reservoir, grey dashed line indicates the outer envelope for two reservoirs in parallel. Colours indicate the moisture index. Note that both axes are limited and the y-axes differ in their range.

Figure S.6 shows the resulting amplitude ratios and phase shifts for the UK and the US together with the ones using E_p as input. Energy-limited catchments (high I_m), in particular the UK catchments, show a similar pattern as when using E_p. The amplitude ratios are slightly higher, i.e. the whole point cloud is slightly shifted to the right. In water-limited catchments in the US, where the annual water balance already implies that $E_a < E_p$, the amplitude ratios are often higher and the phase shifts smaller. Many of the dark red dots that are close to zero in Figure S.6b now plot much further to the right (Figure S.6d). Some of the large phase shifts in these arid catchments might still be a consequence of a poorly estimated input signal. The approach based on the Budyko framework (Equation (B.30)) only reduces the amplitude of the evapotranspiration component, it does not change the timing of E_a compared to E_p. In reality, however, it is possible (and likely) that E_a also has a different phase compared to E_p. Especially in catchments where P and E_p are out of phase, the soil moisture reservoir will fill up during the wet months (peak rainfall) and dry out during the dry months (peak evapotranspiration). If $E_p \gg P$, the soil will likely dry out before we reach peak E_p, and hence we reach peak E_a before peak E_p. The difference in the P peak and the E_p peak (e.g. the phase shift we observe in Figure S.6) would therefore be larger than the difference between the P peak and the E_a peak (i.e. the actual phase shift caused by the catchment). To overcome that, we would either need

modelled E_a, e.g. from a (simple) hydrological model, or measured E_a. Modelling E_a comes at the cost of introducing more modelling steps and therefore more complexity. Measurements of E_a are typically not available at a daily time scale. We therefore leave this for future work.

2.4 Subset of catchments for modelling exercise

The subset of catchments is chosen as follows. We only use benchmark catchments (Harrigan et al., 2018) and remove the catchments with a low flow score of 0 and with any missing values between 1989 and 2009. The remaining set of catchments is manually thinned out to evenly occupy the signature space shown in Figure 5 in the corresponding manuscript. Figure S.7 shows amplitude ratios, phase shifts, and BFIs of the subset.
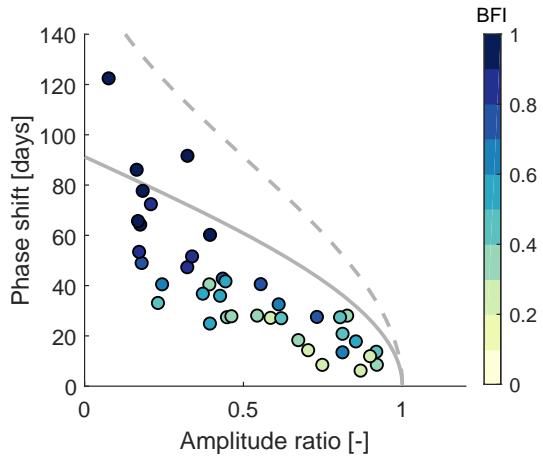
Figure S.7: Amplitude ratio against phase shift for the subset of UK catchments used in the modelling exercise. Grey solid line indicates a single linear reservoir, grey dashed line indicates the outer envelope for two reservoirs in parallel. Colours indicate the BFI.

2.5 Robustness of parameter sampling

To test whether the sample size used in the modelling exercise is large enough, we compare results using different sample sizes. We run the models with 2000, 5000, 10000, and 20000 parameter sets, respectively, all generated using Latin Hypercube sampling. The results from all 40 catchments (see Figure S.7) are summarised using box plots. We then compare the results for different hydrological signatures and different sample sizes. To remove "bad" simulations, we remove parameter sets with a KGE < -0.41 (Knoben et al., 2019). The results are shown in Figure S.8 for IHACRES, and in Figure S.9 for GR4J.

While small differences are visible, the overall the pattern is stable. Since we are interested in the general capabilities of models, rather than individual model runs, we are confident that the parameter space is covered adequately. While sampling more parameter sets is unlikely to change the results, sampling with a different sampling scheme might influence the shapes of the resulting probability distributions.
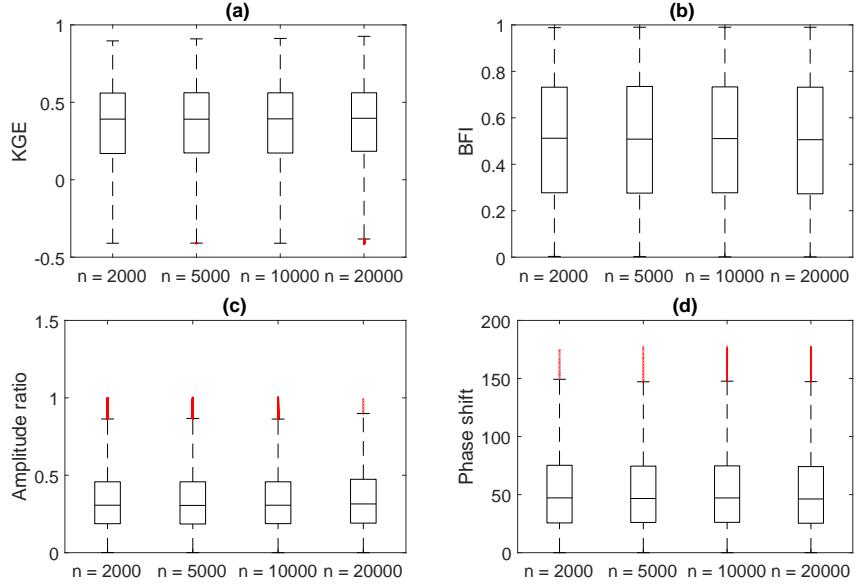
Figure S.8: Box plots summarising model performances for different parameter sample sizes for 40 UK catchments for IHACRES. Boxes indicate the median (middle), the 25th (bottom) and 75th (top) percentiles, respectively. Whiskers show the range of data points not considered outliers. Outliers are shown in red. Performance metrics used are **(a)** KGE, **(b)** BFI, **(c)** the amplitude ratio, and **(d)** the phase shift.
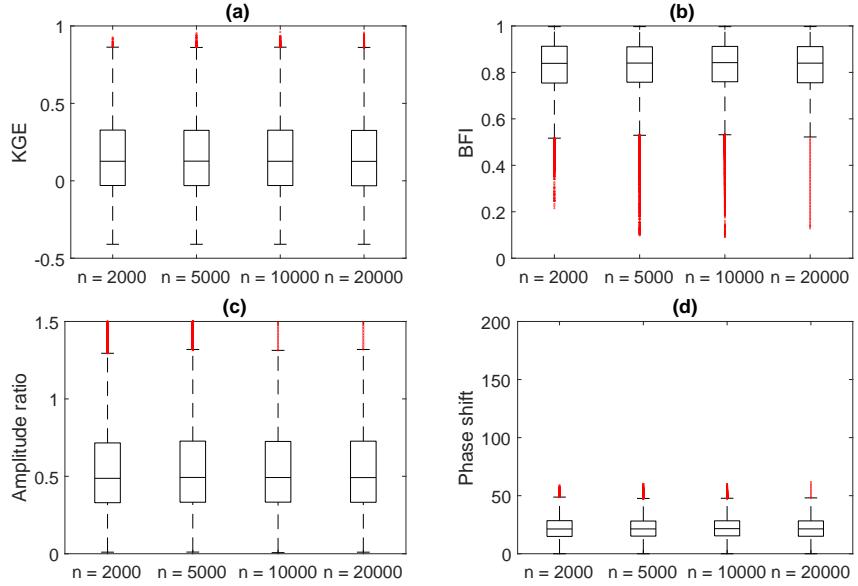
Figure S.9: Box plots summarising model performances for different parameter sample sizes for 40 UK catchments for GR4J. Boxes indicate the median (middle), the 25th (bottom) and 75th (top) percentiles, respectively. Whiskers show the range of data points not considered outliers. Outliers are shown in red. Performance metrics used are **(a)** KGE, **(b)** BFI, **(c)** the amplitude ratio, and **(d)** the phase shift.

References

Budyko, M. I. (1974). *Climate and Life: English Ed. edited by David H. Miller.* Academic Press.

Dooge, J. (1973). *Linear theory of hydrologic systems.* Number 1468. Agricultural Research Service, US Department of Agriculture.

Eriksson, E. (1971). Compartment models and reservoir theory. *Annual Review of Ecology and Systematics*, 2(1):67–84.

Harrigan, S., Hannaford, J., Muchan, K., and Marsh, T. J. (2018). Designation and trend analysis of the updated UK Benchmark Network of river flow stations: the UKBN2 dataset. *Hydrology Research*, 49(2):552–567.

Kirchner, J. W. (2009). Catchments as simple dynamical systems: Catchment characterization, rainfall-runoff modeling, and doing hydrology backward. *Water Resources Research*, 45(2):1–34.

Knoben, W. J. M., Freer, J. E., and Woods, R. A. (2019). Technical note: Inherent benchmark or not? Comparing Nash-Sutcliffe and Kling-Gupta efficiency scores. *Hydrology and Earth System Sciences Discussions*, (July):1–7.

Nash, J. E. (1957). The form of the instantaneous unit hydrograph. *International Association of Scientific Hydrology.*

Peters, E., Torfs, P. J., van Lanen, H. A., and Bier, G. (2003). Propagation of drought through groundwater – A new approach using linear reservoir theory. *Hydrological Processes*, 17(15):3023–3040.

Smith, J. O. (2007). *Introduction to Digital Filters: with Audio Applications*, volume 2. Julius Smith.

Spiegel, M. R. (1968). *Mathematical Handbook of Formulas and Tables.* McGraw-Hill.

Wittenberg, H. (1999). Baseflow recession and recharge as nonlinear storage processes. *Hydrological Processes*, 13(5):715–726.